

# Current Sharing and Critical Current Distribution in Bi-2223 Tapes

F. Hornung, A. Rimikis, and Th. Schneider

**Abstract**—For the applications of technical superconductors, for example in superconducting high-field or NMR magnets, a detailed knowledge of the superconducting-to-normal transition is essential. Usually, this transition is described by a power law leading to the critical current,  $I_C$ , and the  $n$ -value.  $I_C$  and  $n$  are global variables which ignore the microstructure of a superconductor. In contrast, the assumption of a distribution of local critical currents provides a statistical approach to the superconducting-to-normal transition taking into account the non-uniformity of the material.

In this paper, the model of local critical currents is applied to describe the measured voltage-current characteristics of the superconducting transition for several types of Bi-2223 tapes. The probability density of the distribution is evaluated and in addition the current sharing occurring in the transition region between the superconducting phase and the matrix material of the composite is discussed.

**Index Terms**—BSSCO wires, critical current distribution, current sharing, local critical currents, voltage-current characteristics.

## I. INTRODUCTION

THE generation of high magnetic fields is one of the most important applications of superconductors. Magnetic fields well above 20 T can be obtained by superconducting magnets without the massive heat production that occurs in magnets made of normal conducting materials. This reduces the costs for electrical power and cooling. Furthermore, when operating superconducting magnets in persistent mode, i.e. using superconducting joints and a short-circuit by a superconducting switch, an excellent temporal stability of the magnetic field can be obtained.

The high magnetic field laboratory at the Institute for Technical Physics at the Karlsruhe Institute of Technology is engaged in the design, construction, test and operation of superconducting solenoid magnets. The current highlights are the experimental facility HOMER II, setting a world record in 2006 with a field of 20 T in a large bore of 185 mm diameter [1], and, in cooperation with our industrial partners Bruker BioSpin GmbH and Bruker EAS/EHTS GmbH, the world's first 23.5 T/1000 MHz NMR spectrometer, launched onto the market in June 2009 [2]. Until now the magnets of these systems are made

The authors are with the Karlsruhe Institute of Technology, Institute for Technical Physics, Hermann-von-Helmholtz-Platz 1, 76344 Eggenstein-Leopoldshafen, Germany (e-mail: hornung@kit.edu; http://www.itep.kit.edu).

of low temperature superconductors (LTS), namely NbTi and Nb<sub>3</sub>Sn. From today's perspective, for future generations of superconduction magnets with fields of 25 T and above, insert coils built of high temperature superconductors (HTS) have to be used due to the excess of the irreversibility field of the LTS materials.

For the design of such challenging magnet-systems, a detailed knowledge and description of the superconducting-to-normal transition is essential. Usually, this transition is described by a power law  $E(I) = E_C(I/I_C)^n$  leading to the critical current,  $I_C$ , and the  $n$ -value. In this context, the  $n$ -value is a measure for the steepness of the transition, i.e.  $n$  is a differential variable. It should be noted, that  $I_C$  and  $n$  depend on the  $E_C$ -criterion and the  $E$ -interval which is used for determination.

In [3] it was shown, that the  $n$ -value is not adequate to describe in general  $E(I)$ -curves of degraded wires. In addition, an integral method was suggested by evaluating the area  $Q$  under the  $E(I)$ -curve.  $Q$  is a measure for the power dissipation and therefore a useful classification for superconducting transitions. With regard to the application of a wire for NMR magnets, low dissipation is equivalent to a small drift of a magnet.

Nevertheless,  $I_C$ ,  $n$  and  $Q$  are macroscopic variables which ignore the microstructure of a superconductor. For this reason, in this paper, a microscopic model is applied for the description of the superconducting transition of Bi-2223 tapes: the model of local critical currents.

So far, there are only a few experimental studies [4]–[9] in which this model is applied for HTS materials and, as far as we know, there is no concurrent examination of the current sharing between the superconducting phase and the matrix material.

## II. MODEL OF LOCAL CRITICAL CURRENTS

The statistical description of the superconducting transition by the assumption of local critical currents was introduced by BAIXERAS and FOURNET [10] and developed further by several other authors [11]–[15]. The basic idea of this model is that a superconductor can be divided longitudinally in short subsections with each section showing its own local critical current  $i_C^{(j)}$ . The variation of  $i_C^{(j)}$  can be caused by very different reasons such as different pinning strength, saussaging of filaments, grain connectivity, etc.. Assuming ideal type II superconductor flux flow, for  $I > i_C^{(j)}$  the voltage drop  $U^{(j)}$  along the subsection  $j$  is given by

$$U^{(j)}(I, B, T) = R^{(j)}(B, T) \left( I - i_C^{(j)}(B, T) \right). \quad (1)$$

Note that in the experiments discussed here, thermally activated vortex motion can be neglected due to the cooling of the HTS-superconductor in helium at  $T = 4.2$  K, i.e.  $T \ll T_C$ .

TABLE I  
PROPERTIES OF THE INVESTIGATED Bi-2223 TAPES

	Sample A	Sample B
Production year	ca. 1998	2008
Dimensions	3.5 mm × 0.25 mm	4.5 mm × 0.34 mm
Filaments	55	unknown
Supercond. fraction	30%	40%
Matrix	Ag	Ag
Sheath	AgMg	Ag-alloy
Lamination	none	copper alloy (50 μm × 2)

Due to current sharing, a part of the excess current  $I - i_C^{(j)}$  flows in the normal conducting matrix of the technical superconductor. Therefore, the resistance  $R^{(j)}$  of the subsection is given by the parallel connection of the matrix and the superconducting phase. Note, in this paper, ‘matrix’ implies the complete non-superconducting metallic shunt, i.e. the actual matrix embedding the filaments plus the encasing sheath.

For a large number of subsections, the variation of  $i_C^{(j)}$  changes to the probability density  $\phi(i_C)$  of local critical currents. Integration leads to the resulting voltage  $U$  across the whole measuring length  $L$

$$U(I, B, T) = R^*(B, T) \int_0^I (I - i_C(B, T)) \phi(i_C) di_C \quad (2)$$

where the resistance  $R^*(B, T)$  is determined according to (4) by the ohmic matrix,  $R_{\text{ma}}$ , and the flux flow in the superconducting phase  $R_{\text{ff}}$ . Differentiating (2) twice and switching to the electrical field  $E(I, B, T) = U(I, B, T)/L$  results in

$$\frac{d^2 E(I, B, T)}{dI^2} = r^*(B, T) \phi(i_C) \quad (3)$$

with

$$r^* \equiv \frac{R^*}{L} = \left( \frac{L}{R_{\text{ff}}} + \frac{L}{R_{\text{ma}}} \right)^{-1} \equiv \left( \frac{1}{r_{\text{ff}}} + \frac{1}{r_{\text{ma}}} \right)^{-1}. \quad (4)$$

### III. EXPERIMENTAL AND DATA PROCESSING

The experiments were carried out in the facility JUMBO [16] in external magnetic fields up to 10 T at a helium bath temperature of 4.2 K. Several one layer test coils were wound with diameters of 90 mm made of Ag/Ag-alloy Bi-2223 tapes from different manufacturers. Details on these wires can be found in Table I. For these samples, the  $E(I)$ -characteristics were examined using the so-called ‘step-and-hold’-technique. After a discrete current step there is a delay of several seconds before measurement of the voltage under quasi steady-state conditions in a resistive high resolution four-point configuration [17].

According to (3), for the determination of the probability density of the local critical currents  $\phi(i_C)$ , the measured  $E(I)$  data set has to be differentiated twice. For this, a modification of the SAVITZKY and GOLAY method was applied: An interval of  $m = 2p + 1$  data points was fitted in our case by a linear polynomial to get the slope at the midpoint of the interval. By shifting

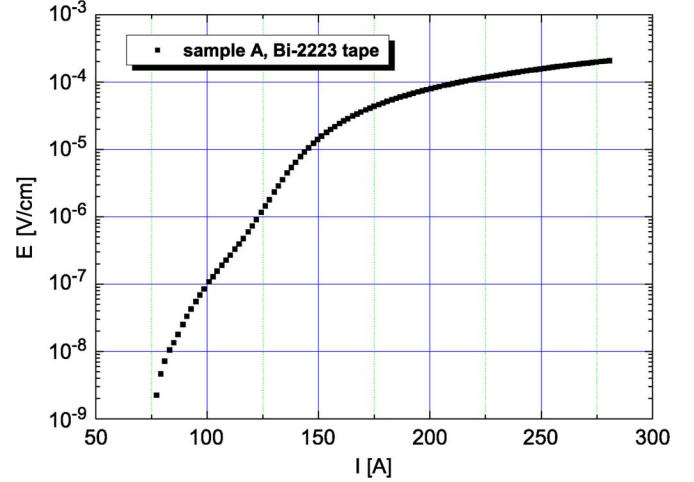


Fig. 1. Logarithmic plot of  $E(I)$  measured for a Ag/AgMg Bi-2223 tape manufactured in 1998 (sample A) at 4.2 K and an external field of 0.5 T.

the interval point by point through the data set, the first derivative is obtained. To get the second derivative, this procedure was rerun for the data set obtained for the first derivative. It turned out, that for our measurements  $m$  in the range of 7 to 15 is a good compromise between smoothing and maintaining details in the derivatives.

## IV. RESULTS AND DISCUSSION FOR SAMPLE A

### A. Distribution of Local Critical Currents

In Fig. 1 the  $E(I)$ -curve measured at 4.2 K for sample A which was manufactured in ca. 1998 is given. For reasons of clarity, we concentrate on the data obtained for  $B = 0.5$  T. Measurements for other magnetic fields were also performed, but are not shown, as they give no additional information for the context discussed in this paper. The low magnetic field of 0.5 T has the advantage that the influence of magneto-resistance can be neglected.

The classical evaluation of the  $E(I)$ -curve with respect to  $I_C$  and  $n$  gives  $I_C = 100.2$  A for a  $E_C$ -criterion of  $10^{-7}$  V/cm and  $n = 11.2$  at  $I(E_C)$ . Both values are rather low compared to today’s perspective, but typical for Bi-2223 wires manufactured about 10 years ago.

For a technical Bi-2223 superconductor with a low-resistance shunt (in this case the matrix/sheath of Ag/AgMg) for  $I \gg I_C$  the voltage-current characteristics is dominated by the shunt as the flux flow resistance can be estimated to be 2-3 orders of magnitude larger [18]. Hence  $r^* \rightarrow r_{\text{ma}}$ . Therefore,  $r_{\text{ma}}$  is given by the slope of the (linear) asymptotic behavior of  $E(I)$  in Fig. 2:  $r_{\text{ma}} = 1.59 \times 10^{-6}$  Ω/cm. By considering the cross-sectional area of the tape and the filling factor, the effective resistivity of the non-superconducting area (i.e. matrix plus sheath) is calculated to be  $\rho = 9.75 \times 10^{-9}$  Ωcm. This value corresponds to a residual resistance ratio of  $RRR = 164$  when compared to the resistivity of pure Ag.

The second derivative of the  $E(I)$ -data shown in Fig. 1 is given in Fig. 3. It turns out that the complete probability density  $\phi(i_C)$  of local critical currents is experimentally accessible. This

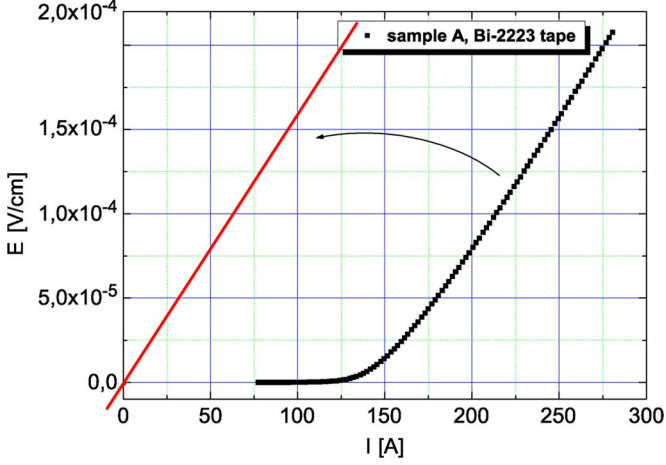


Fig. 2. Determination of the resistance load per unit length,  $r_{\text{ma}}$ , of the matrix of sample A from the slope of the linear asymptote of  $E(I)$ :  $r_{\text{ma}} = 1.59 \times 10^{-6} \Omega/\text{cm}$ .

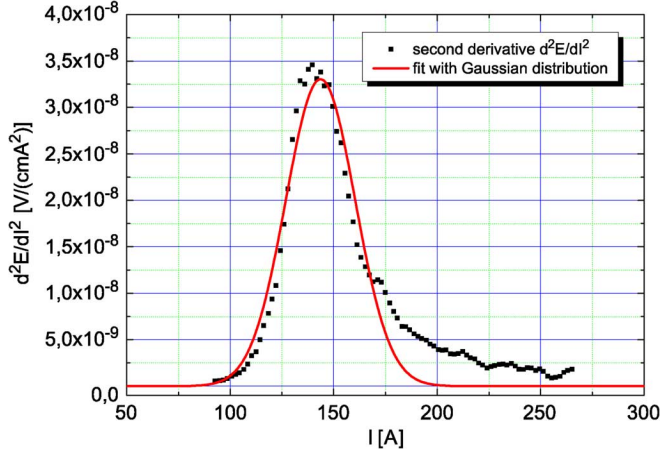


Fig. 3. Second derivative of  $E(I)$  measured for sample A (squares, see Figs. 1 and 2).  $d^2E(I)/dI^2$  can be very well described by a Gaussian probability density of local critical currents (line).

is not the normal case as a review of the literature shows. Apart from exceptions, for LTS and HTS only a part of the left tail could be measured [7], [9], [19].

According to (3), the integral of  $d^2E(I)/dI^2$  equals  $r^*$ . For the area under the second derivative of  $E(I)$  in Fig. 3 (squares) one gets  $r^* = 1.62 \times 10^{-6} \Omega/\text{cm}$ . This agrees very well with the value obtained for  $r_{\text{ma}}$  from the slope of the asymptote of  $E(I)$  in Fig. 2. Apparently, the calculation of the second derivative using the above described modified SAVITZKY-GOLAY method is reliable.

In literature, a GAUSS distribution is often used to fit the measured  $d^2E(I)/dI^2$  data. This corresponds to the assumption that the local critical currents originate from a large number of independent causes. Fig. 3 shows a GAUSS-fit to the second derivative of  $E(I)$ . The fit matches quite well. The values of the three free parameters are area  $A = 1.39 \times 10^{-6} \Omega/\text{cm}$ , mean value  $\mu = 143.6$  A, and standard deviation  $\sigma = 16.8$  A. Compared to  $r^*$ , the area is somewhat underestimated by the fit as the right tail of the distribution is not described accurately.

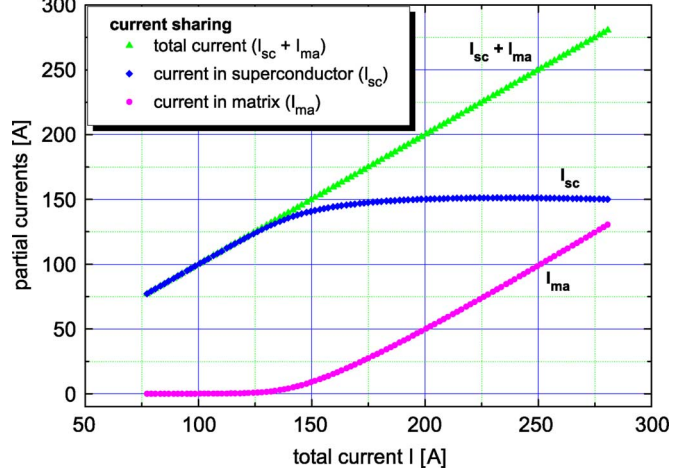


Fig. 4. Current sharing between the matrix and the superconducting branch determined for sample A at 4.2 K and an external field of 0.5 T. The partial currents are plotted versus the total current flowing in the composite. At about  $1.90I_C (= 190$  A) the superconducting branch is completely saturated and the additional current is carried by the matrix only.

## B. Current Sharing

The superconducting filaments are connected electrically in parallel with the matrix. Therefore, the following relationships are valid:

$$E(I) = r_{\text{sc}}(I_{\text{sc}})I_{\text{sc}} = r_{\text{ma}}I_{\text{ma}} \quad \text{and} \quad I = I_{\text{sc}} + I_{\text{ma}}. \quad (5)$$

The indices ‘sc’ and ‘ma’ refer to the superconducting material and to the metallic matrix, respectively. Variables without an index refer to the total composite.

From (5), the current sharing between the superconducting filaments and the matrix can be calculated as shown in Fig. 4. Below  $1.25I_C (= 125$  A) more than 99% of the current is carried by the superconductor. On reaching this value, the current flow in the matrix increases strongly. At about  $1.90I_C (= 190$  A) the superconducting branch is completely saturated and from this point the additional current is carried by the matrix of the composite only. The cause of the current sharing is the exceeding of local critical currents: In fact, the comparison of Figs. 3 and 4 shows that the region where additional current is distributed between the two branches is identical to the region where  $d^2E(I)/dI^2 > 0$ .

The dissipation per length for the two branches is given by  $p_{\text{sc}} = E \times I_{\text{sc}}$  and  $p_{\text{ma}} = E \times I_{\text{ma}}$ , respectively. Fig. 5 shows the developing of this dissipation together with the value for the whole composite. All curves are plotted versus the total current flowing in the composite. It should be emphasized that for the whole investigated current range the dissipation in the superconducting branch is larger than the one in the matrix. The maximum dissipation can be calculated from Fig. 5 to  $0.058$  W/cm, i.e.  $0.167$  W/cm<sup>2</sup>. This leads to a temperature rise of the tape of maximal 0.47 K according to the conservative estimation of heat-transfer given in [20]. Therefore, the sample is in the nucleate-boiling regime of helium during the complete measurement.

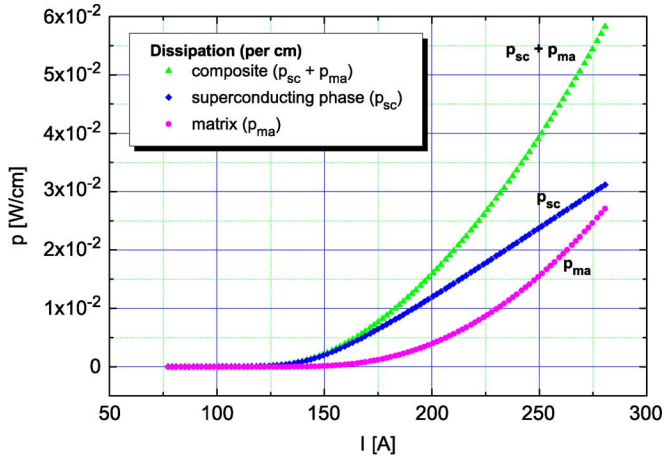


Fig. 5. Dissipation per length for the normal- ( $p_{ma}$ ) and superconducting ( $p_{sc}$ ) branch of sample A at 4.2 K and an external field of 0.5 T. For the whole investigated current range the dissipation in the superconducting branch is larger than that in the matrix.

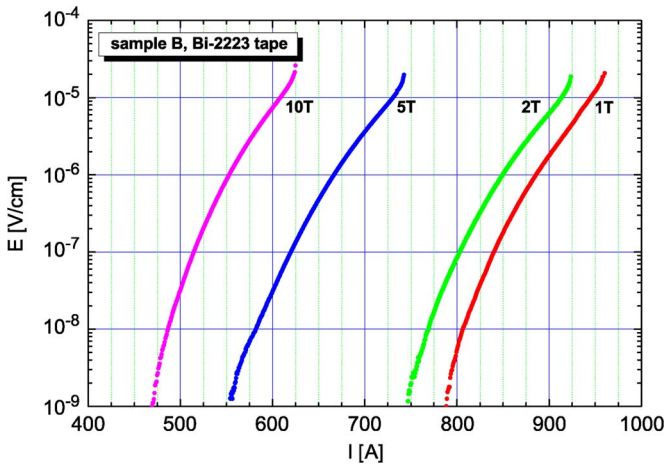


Fig. 6. Logarithmic plot of  $E(I)$  measured for a Ag/Ag-alloy Bi-2223 tape manufactured in 2008 (sample B) at 4.2 K and various external magnetic fields. In contrast to sample A (see Fig. 1) there is a upturn instead of a flattening in the log-plot of the  $E(I)$ -curves for high currents.

## V. RESULTS AND DISCUSSION FOR SAMPLE B

The investigations carried out for sample A were repeated for several up-to-date Bi-2223 tapes of different manufacturers and the results obtained are represented by the data for sample B (see Table I). Fig. 6 shows the  $E(I)$ -curves measured for various external magnetic fields at 4.2 K. In contrast to sample A (see Fig. 1) there is no flattening in the log-plots of  $E(I)$  for high currents. Instead, the curves turn up ending with a quench of the sample for all runs. This behavior is typical for state-of-the-art samples. It should be noted that the dissipation right before the quench is considerably lower compared to the maximum dissipation of sample A.

For such  $E(I)$ -curves only a part of the left tail of the probability density  $\phi(i_C)$  of local critical currents is experimentally accessible and a 3-parameter GAUSS-fit to  $d^2E(I)/dI^2$  delivers non-physical results with large error margins. This reiterates the issue reported in papers when investigating  $\phi(i_C)$  of LTS [7],

[9], [19]. Furthermore, a reduction to two free parameters by fixing the value of  $r^*$ , i.e. the area  $A$  of the fit, is not possible because  $E(I)$  cannot be linearly extrapolated as in the case of sample A (see Fig. 2).

## VI. CONCLUSION

The voltage-current relation  $E(I)$  of several Ag/Ag-alloy Bi-2223 tapes from different manufacturers was analysed with regard to the underlying probability density  $\phi(i_C)$  of local critical currents  $i_C$ . For a sample originating from the early days of the Bi-2223 fabrication, the complete probability density was experimentally accessible.  $\phi(i_C)$  could be very well described by a GAUSS-fit. Furthermore, the current sharing between matrix and superconducting phase was analysed. Firstly,  $E(I)$  is dominated by the superconducting phase, followed by a transition region, before  $E(I)$  is determined by the matrix for  $I \gg I_C$ . To our knowledge, this is the first time, current sharing and the distribution of local critical currents has been investigated simultaneously for the same Bi-2223 sample. In contrast, due to the upturn of  $E(I)$  followed by a quench, the analysis described above cannot be performed for state-of-the-art Bi-2223 tapes. This resembles to the situation reported in papers dealing with  $\phi(i_C)$  of LTS. The reasons for the different behavior of the two generations of Bi-2223 tapes are currently under investigation.

## REFERENCES

- [1] T. Schneider, M. Beckenbach, R. Ernst, F. Hornung, M. Kläser, H. Lahn, P. Leys, H. Neumann, C. Ruf, and M. Stamm, *IEEE Trans. Appl. Supercond.*, submitted for publication.
- [2] Bruker BioSpin GmbH, Germany, Press release Jun. 1st 2009 [Online]. Available: <http://www.bruker.biospin.com/pr090601.html>, Available
- [3] F. Hornung, M. Kläser, and T. Schneider, *IEEE Trans. Appl. Supercond.*, vol. 17, pp. 3117–3120, 2007.
- [4] F. Irie, Y. Tsujioka, and T. Chiba, *Supercond. Sci. Technol.*, vol. 5, pp. S379–382, 1992.
- [5] M. Mimura *et al.*, *Advances in Superconductivity*. Tokyo: Springer, 1997, vol. 10, pp. 747–750.
- [6] H. Okamoto, F. Irie, T. Kiss, M. Inoue, and M. Kanazawa, *Supercond. Sci. Technol.*, vol. 12, pp. 1102–1105, 1999.
- [7] R. Kimmich, A. Rimikis, and T. Schneider, *IEEE Trans. Appl. Supercond.*, vol. 9, pp. 1759–1762, 1999.
- [8] K. Osamura, K. Ogawa, T. Thamizavel, and A. Sakai, *Physica C*, vol. 335, pp. 65–68, 2000.
- [9] H. Müller, F. Hornung, A. Rimikis, and T. Schneider, *IEEE Trans. Appl. Supercond.*, vol. 17, pp. 3757–3760, 2007.
- [10] J. Baixeras and G. Fournet, *J. Phys. Chem. Solids*, vol. 28, pp. 1541–1547, 1967.
- [11] W. H. Warnes and D. C. Larbalestier, *Cryogenics*, vol. 26, pp. 643–653, 1986.
- [12] D. P. Hampshire and H. Jones, *Cryogenics*, vol. 27, pp. 608–616, 1987.
- [13] C. J. G. Plummer and J. E. Evetts, *IEEE Trans. Mag.*, vol. 23, pp. 1179–1182, 1987.
- [14] W. H. Warnes, *J. Appl. Phys.*, vol. 63, pp. 1651–1662, 1988.
- [15] S. Takács, *Cryogenics*, vol. 28, pp. 374–380, 1988.
- [16] A. Rimikis, F. Hornung, and T. Schneider, *IEEE Trans. Appl. Supercond.*, vol. 10, pp. 1542–1545, 2000.
- [17] H. Leibrock, F. Hornung, M. Kläser, H. Müller, and T. Schneider, *Physica C*, vol. 401, pp. 255–259, 2004.
- [18] T. Aritake, T. Noda, H. Shimizu, Y. Yokomizu, T. Matsumura, and N. Murayama, *IEEE Trans. Appl. Supercond.*, vol. 13, pp. 2084–2087, 2003.
- [19] R. Kimmich, *Wissenschaftliche Berichte*. Karlsruhe, Germany: Forschungszentrum Karlsruhe, 2001, FZKA 6562.
- [20] C. Schmidt, *Stability of Superconductors*. Saclay, France: International Institute Refrigeration. Commission A 1/2, 1981, pp. 17–32.